

AD-A067 212

UNIVERSITY OF SOUTHERN CALIFORNIA LOS ANGELES
SURFACE WAVE RESONATOR AND BULK WAVE CRYSTAL FILTERS. (U)
MAR 79 K M LAKIN

F/6 9/5

UNCLASSIFIED

ARO-13527.1-EL

DAA629-76-G-0166

NL

|OF|
AD
A067212



END
DATE
FILMED
6-79

DDC

AD A0 67212

DDC FILE COPY

ARO 13527.1-EL

12

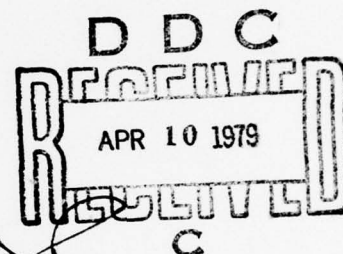
LEVEL

SURFACE WAVE RESONATOR AND
BULK WAVE CRYSTAL FILTERS

FINAL REPORT

K. M. Lakin

12 March 1979



U.S. ARMY RESEARCH OFFICE

GRANT DAAG29 76 G 0166

Period

1 April 1976 - 30 November 1978

University of Southern California
Los Angeles, California 90007

APPROVED FOR PUBLIC RELEASE; DISTRIBUTION UNLIMITED

79 04 09 099

Unclassified

SECURITY CLASSIFICATION OF THIS PAGE (When Data Entered)

REPORT DOCUMENTATION PAGE		READ INSTRUCTIONS BEFORE COMPLETING FORM
1. REPORT NUMBER None	2. GOVT ACCESSION NO.	3. RECIPIENT'S CATALOG NUMBER
4. TITLE (and Subtitle) Surface Wave Resonator and Bulk Wave Crystal Filters	5. TYPE OF REPORT & PERIOD COVERED FINAL repl 1 Apr 76-30 Nov 78	6. PERFORMING ORG. REPORT NUMBER
7. AUTHOR(s) K. M. Lakin	8. CONTRACT OR GRANT NUMBER(s) DAAG29-76-G-0166	9. PERFORMING ORGANIZATION NAME AND ADDRESS University of Southern California Los Angeles, Calif. 90007
10. CONTROLLING OFFICE NAME AND ADDRESS U. S. Army Research Office P. O. Box 12211 Research Triangle Park, NC 27709	11. REPORT DATE Mar 1979	12. NUMBER OF PAGES 37
13. MONITORING AGENCY NAME & ADDRESS (if different from Controlling Office) ARO 13527.1-EL	14. SECURITY CLASS. (of this report) Unclassified	15. DECLASSIFICATION/DOWNGRADING SCHEDULE
16. DISTRIBUTION STATEMENT (of this Report) Approved for public release; distribution unlimited.		
17. DISTRIBUTION STATEMENT (of the abstract entered in Block 20, if different from Report) N/A		
18. SUPPLEMENTARY NOTES The view, opinions, and/or findings contained in this report are those of the author(s) and should not be construed as an official Department of the Army position, policy, or decision, unless so designated by other documentation.		
19. KEY WORDS (Continue on reverse side if necessary and identify by block number) Surface wave, resonators, bulk wave, crystal filters		
20. ABSTRACT (Continue on reverse side if necessary and identify by block number) This report details a 32 month research project on surface acoustic wave, SAW, two port resonator filters, phase weighted gratings for surface wave resonators, and the equivalent circuit modeling of a thin film stacked crystal bulk wave filter. The report details a new device configuration for coupled two port SAW resonators which would allow the coupling to occur only when the grating reflectors are in resonance and would offer little coupling when the resonator is out of the resonance condition. This configuration is		

composed of an interdigital electrode transducer, IDT, which is placed within the grating itself but is an IDT whose periodicity is an even multiple of the wavelength.

The concept of a phase weighted grating is described for use in wide band resonators. This new concept is based upon the unique properties of gratings and the concept of a movable reflection plane.

A simple equivalent circuit for the thin film stacked crystal filter is derived for the first time and results in a lumped element representation for this important device.

ACCESSION for	
NTIS	Whole Section <input checked="" type="checkbox"/>
GDC	Part Section <input type="checkbox"/>
UNANNOUNCED	
DISSEMINATION	
BY DISTRIBUTION/AVAILABILITY CODES	
DI	SPECIAL
A	

TABLE OF CONTENTS

1.0 INTRODUCTION	1
1.1 Scope	1
1.2 Background	1
2.0 RESEARCH TASKS	2
2.1 Goals	2
2.2 Description and Results	2
2.2.1 Photomask Production	2
2.2.2 Automatic Network Analyzer	5
2.2.3 Modeling and Display	6
2.2.4 Two-Port Resonator Feedthru	7
2.2.5 Phase Weighted Grating Resonators	14
2.2.6 Two Port Bulk Wave Filters	17
3.0 SUMMARY AND CONCLUSIONS	31
4.0 REFERENCES	33

LIST OF ILLUSTRATIONS

Figure		Page
2.1	Two Port Resonator	8
2.2	Insertion Loss of Two-Port Resonator.	9
2.3	Wave Amplitude Versus Distance	11
2.4	IDT Coupled Grating.	13
2.5	Stacked Crystal Filter Schematic	18
2.6	Mason Equivalent Circuit	21
2.7	SCF With Zero Bond Thickness	22
2.8	Equivalent Pi Network for SCF	24
2.9	SCF Lumped Equivalent Circuit	26
2.10	SCF, Crystal Film Implementation	29

1.0 INTRODUCTION

1.1 Scope

This report covers a two year plus eight month extension period on a grant studying two port surface acoustic wave, SAW, filters, a new form of phase weighted grating and a two port filter configuration employing bulk waves. This later device, a thin film form of the stacked crystal filter, SCF, was introduced during the last year of the program.

The various topics were chosen in order to maximize the impact on our program and the SAW resonator field in general. These decisions were made at the start of the program and during the last year of the effort. Over the 32 month period of the program four first year students were involved in the program at one time or another; although no more than one at a time, except during the last year when two were engaged in the two port stacked crystal filter research. Of the four, one went to industry after one year and two are now working on their Ph.D. degrees at USC in the area of stacked crystal filters or bulk wave transduction.

1.2 Background

The original work on SAW resonators at USC was under the sponsorship of the Joint Services Electronics Program, JSEP, and was funded under the general topical heading "Surface Wave Propagation Studies". At the same time as the USC work a major effort was also going on in industry unknown to us [1]. However, based upon the work published and done at USC [2, 3, 4] we proposed a major program on SAW resonator research in July of 1975 and by September of that year all resonator work at USC

had ceased. By the time this program started, in April 1976, the major contributor to our work, Mr. T. Joseph, had graduated and the new SAW resonator research area had exploded with researchers and published papers. By this time much of the straightforward work we had proposed had already been done or was no longer relevant.

Nevertheless, important areas still needed to be studied and we concentrated our attention on the two port resonator feedthru problem, the phase weighted grating, and, toward the end of the program, the crystal film bulk wave two port stacked crystal filter.

This report details the tasks that were studied and the progress made during the 32 month research period.

2.0 RESEARCH TASKS

2.1 Goals

Starting with completely new personnel and somewhat late in the then now, well established SAW resonator field, it was decided that a maximum impact could be made by attacking the problem of the large out-of-band feedthru experienced in two port resonators. To accomplish this we had to automate the resonator mask making procedure so that unstrained operators could produce usable devices, automate the network analyzer in order to increase the speed and precision of resonance and filter passband measurements, and finally, to aid the grating and resonator modeling by putting the programs on the new Tektronix graphics micro-computer. It was felt that this would be an ideal program to train new students in the art and science of SAW devices and precision measurements as well as accomplish the research goals.

Late in the program, after we had little success with SAW resonators due to mask making problems, our attention was shifted to the bulk wave counterpart of the SAW two port resonator, the stacked crystal filter, SCF. We had firmly laid the groundwork for this latter research by the end of this program.

What follows next is a description of the work involved and progress made on these tasks.

2.2 Description and Results

2.2.1 Photomask Production

An essential feature of the proposed program was to study new

resonator devices and the resonance phenomena. As outlined in the introduction, this would require devices of size and complexity that could not be cut out manually on the coordinator graph as had been done in our JSEP work. We decided that it would be sufficient to build an inexpensive step and repeat plate holder for the back of the existing 50X reduction camera and then control the stepper with the Tektronix 4051 through the IEEE 488 interface bus. The plate holder was designed around a four inch diameter and five inch long aluminum tube. The plate holder was attached to this tube with differential screws formed by two threaded collars. A one half inch turn along the circumference of the inner collar then advanced the photo plate five microns. The XY tables were then mounted to the camera body through an adaptor and the plate holder was then attached to the Y table. The result was a stepping interval of 10 micro inches over an area of 2"x2".

A considerable amount of effort was required to aline the plate holder to the camera so that the plate would be parallel to the object plane of the camera backboard. This procedure was carried out largely by trial and error but has now become a simple task.

The computer interface was a somewhat time consuming task because of a lack of documentation for the numerical controller used to drive the stepping motors. Eventually the ICON 350 controller was appropriately modified and the step and repeat system was under computer control near the end of the first year.

This instrument proved a major asset in that a SAW resonator mask

could be easily made in one day or less and required only simple loop programming of less than 20 lines of code. However, we eventually found that it was not accurate enough for SAW resonator work due to a periodic error in the lead screw. Close to one hundred photomasks were made on this instrument during the entire extent of the program, most of the photomasks were made for this research program and the remainder for other research programs at USC.

2.2.2 Automatic Network Analyzer

One of the requirements of SAW resonator research is a large number of precision measurements of the magnitude and phase of either impedance or reflection coefficient as a function of frequency. Further, in a cavity loaded by an IDT transducer, the one port resonator Q must be determined by a measurement of the slope of the phase of impedance or admittance. However, our previous experience indicated that the impedance probe loaded the IDT and gave readings that were difficult to interpret. Instead the impedance must be inferred from a measurement of the complex reflection coefficient and converted by the usual formula. Since all these procedures must be carried out at each frequency, the measurement task becomes a major chore. Thus we took steps to completely computer control the measurement process.

A key element in the computer control of the network analyzer was the Wavetek 3000 frequency synthesizer that was purchased on the program. Again this device required an appropriate interface in order for the computer to control the experiment. The procedure then is for the computer to set

the frequency on the synthesizer and then read a digital voltmeter connected to the analog magnitude and phase outputs of the network analyzer. Once the data was in the computer it could be analyzed to give the data of interest.

About half of this task was supported by another program which also required the network analyzer for control purposes.

2.2.3 Modeling and Display

The kind of device modeling that had been carried out in our previous work involved the fitting of theoretical data to experimental results in order to determine the modeling parameter for the given device configuration and known physical dimensions. For example, although the stripe width, stripe to gap width ratio, and stripe thickness could all be measured, the effect of the grating upon the propagating wave could not be determined directly. However, by an accurate modeling, the impedance discontinuity parameter could be obtained by curve fitting at one or two points and then the entire curve mapped out by the theory. Our original work along these lines involved a punched card input computer system (IBM 370) with output in the form of line printer plots. The turn around time for such a procedure could be as long as two days but rarely shorter than one-half day. However, once having the 4051 graphics system in hand the computing picture changed drastically.

In order to implement the modeling under local control we purchased on grant funds a data communications adaptor which allowed the 4051 to interface directly with a large mainframe computer, DEC PDP KL10, over a 2400 baud data line. To give a hard copy we also purchased a hard copy

unit which produces copies of both graphs and programs.

This system proved to be useful and flexible for doing the resonator type calculations in that either the large computer could be used or the Tektronix 4051 itself. Usually the 4051 was used by itself at considerable savings in computer time. The turn around time for a simple resonator plot could be less than one hour depending on how precise a graph was required.

The main expense in time for this task was in the initial writing and debugging of computer programs since it is not really practical to try to convert Fortran to Basic although the reverse is relatively easy.

2.2.4 Two Port Resonator Feedthrough

In Figure 2.1 is shown the basic features of a two-port resonator composed of two gratings to form a resonant cavity and two transducers to couple energy in and out of the cavity. The basic principle is like that of any coupled cavity where there is a chance of direct coupling from input to output. In Figure 2.2 is shown a typical frequency response for a two port SAW resonator. Note in particular the large level of feedthru outside the main resonance peaks. This feedthru is due to the two transducers acting as a relatively simple delay line at those frequencies where the gratings are transparent. Whereas a single two port resonator may give a satisfactory in-band insertion loss the out-of-band signal levels are not acceptable for a good filter response. This feature is a major problem with SAW resonators and a number of configurations which might have overcome this problem were discussed in the proposal for this program. However,

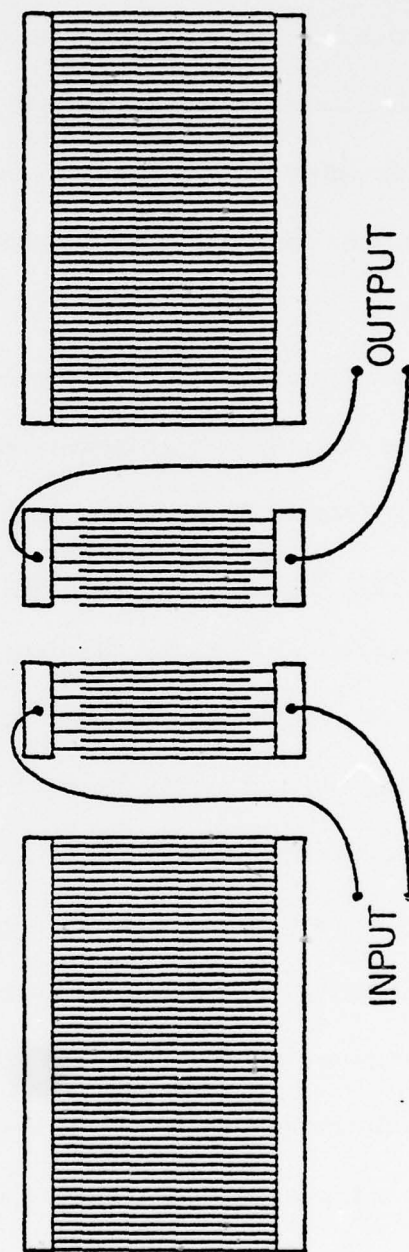


Figure 2.1 Two-port resonator.

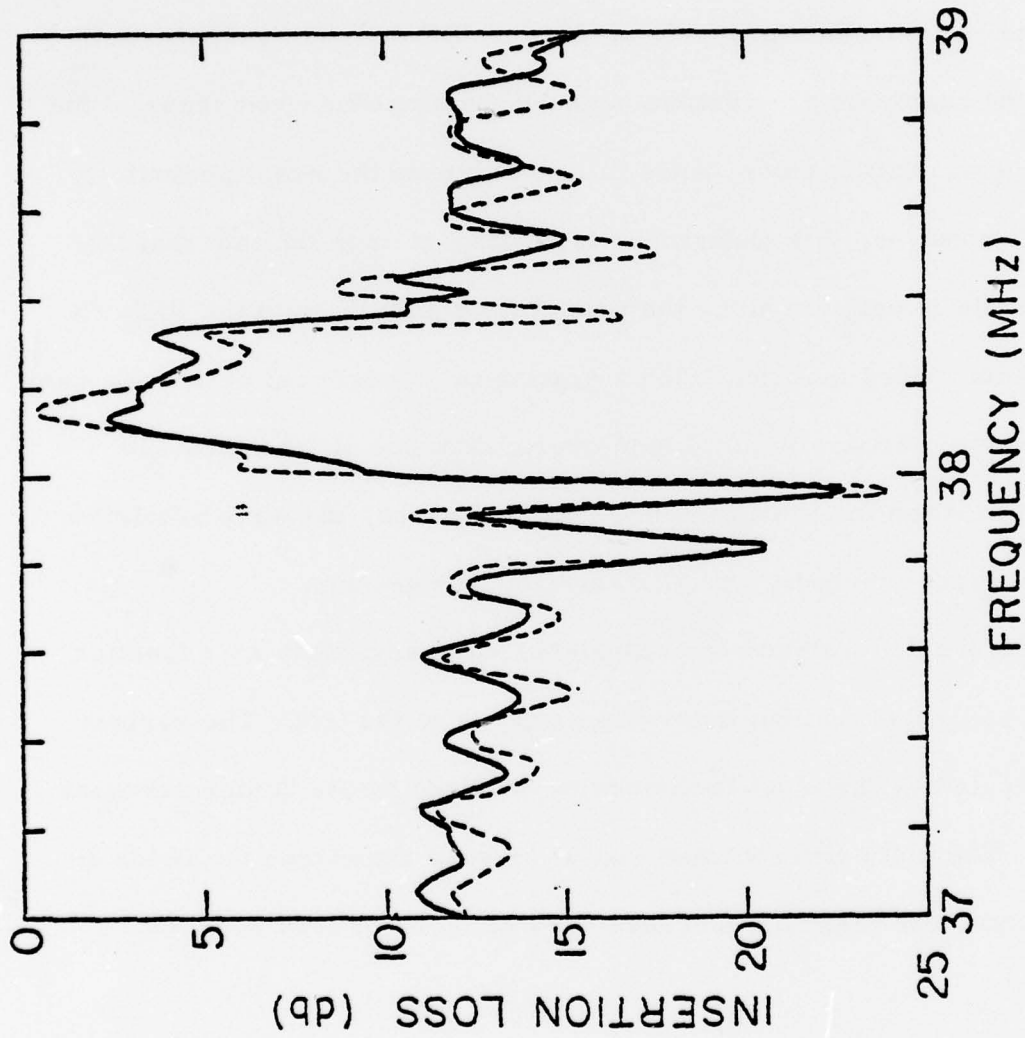


Figure 2.2 Insertion loss of a two-port resonator.

for reasons stated before we decided to confine our attention to one such approach which would require at most two coupled cavities to accomplish the desired results.

The particular device configuration that was considered for the two port resonator configuration exploits a fundamental property of interdigital transducers. This property is that the IDT does not respond well at its second harmonic or overtone because the amplitude and phase of the standing or propagating waves tends to cancel due to the exact periodicity mismatch. However, this phenomena is contingent upon the fact that the wave amplitude is uniform along the propagation path through the IDT. It is also an established fact that when a grating is strongly reflecting the wave amplitude rapidly decays in amplitude over a distance of less than 100 wavelengths. When the grating is not near resonance, the wave amplitude does not decrease markedly with distance into the grating.

In Figure 2.3 we show the calculated wave amplitude as a function of distance along the grating; hence the cavity is to the left. The various plots are labeled by the input frequency normalized by the center resonant frequency. The plots clearly show that at or near resonance the fields do drop off rapidly and that off resonance assume more or less constant amplitude.

Thus the thought occurred to us to put an IDT structure within the grating such that its periodicity was an even multiple of the wavelength and would look like an IDT at one-half the grating resonant frequency. Therefore, when the grating is not near resonance the IDT would not

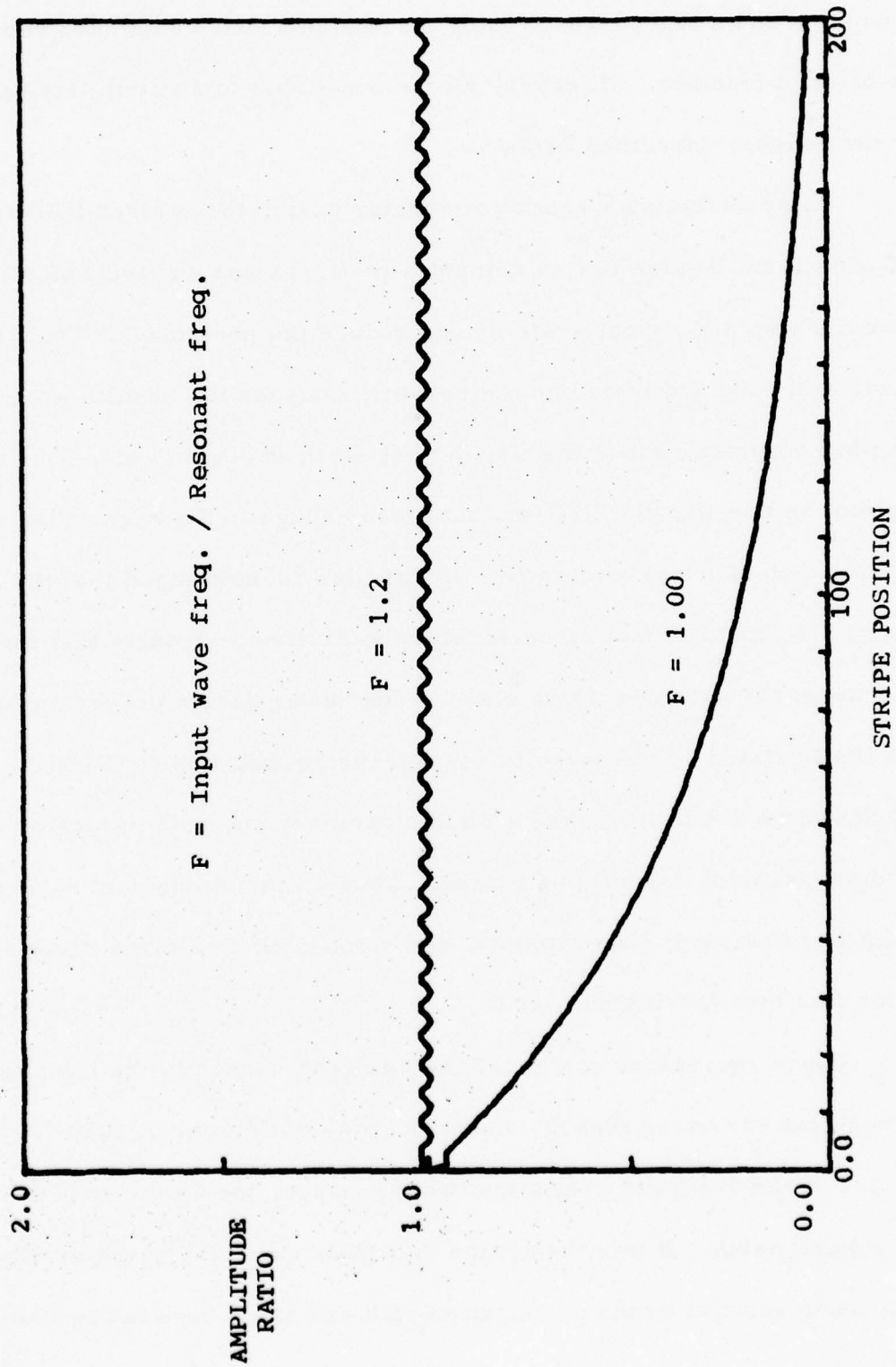


Figure 2.3 Normalized wave amplitude versus stripe position in the grating.

couple well and when the grating was in resonance the IDT would couple energy the strongest. In this manner it appeared that two cavities could be coupled and a two port resonator fabricated which would have very low out-of-band feedthru. However, we were not able to confirm this operation for the reasons described below.

After designing a grating resonator having the desired interspersed IDT structure, Figure 2.4, a computer program was written which would drive the step and repeat system and produce the photomask. Once having a device in hand and tested on the network analyzer the results were anything but optimistic since the IDT did not seem to couple well. Our first assumption was that the IDT was not close enough to the edge of the cavity and so a redesign was attempted. It was also acknowledged that the intergrating IDT could in fact be perturbing the cavity so strongly that the resonance was not even taking place. The newer design proved no better than the first and so we began to suspect the grating itself. Finally, as a self check we decided to make a simple ordinary one port resonator as we had demonstrated many times before. Thus a simple one port resonator cavity was designed, programmed, and stepped off to make a mask and the device was then fabricated.

Since resonators can rarely be designed correctly the first time we were not surprized that the resonance was not correct. After several changes in the design to maximize the resonance, the Q was still way below the desired value. It was then found that there was a very subtle tilt in the grating relative to the propagation path and since the grating lines were

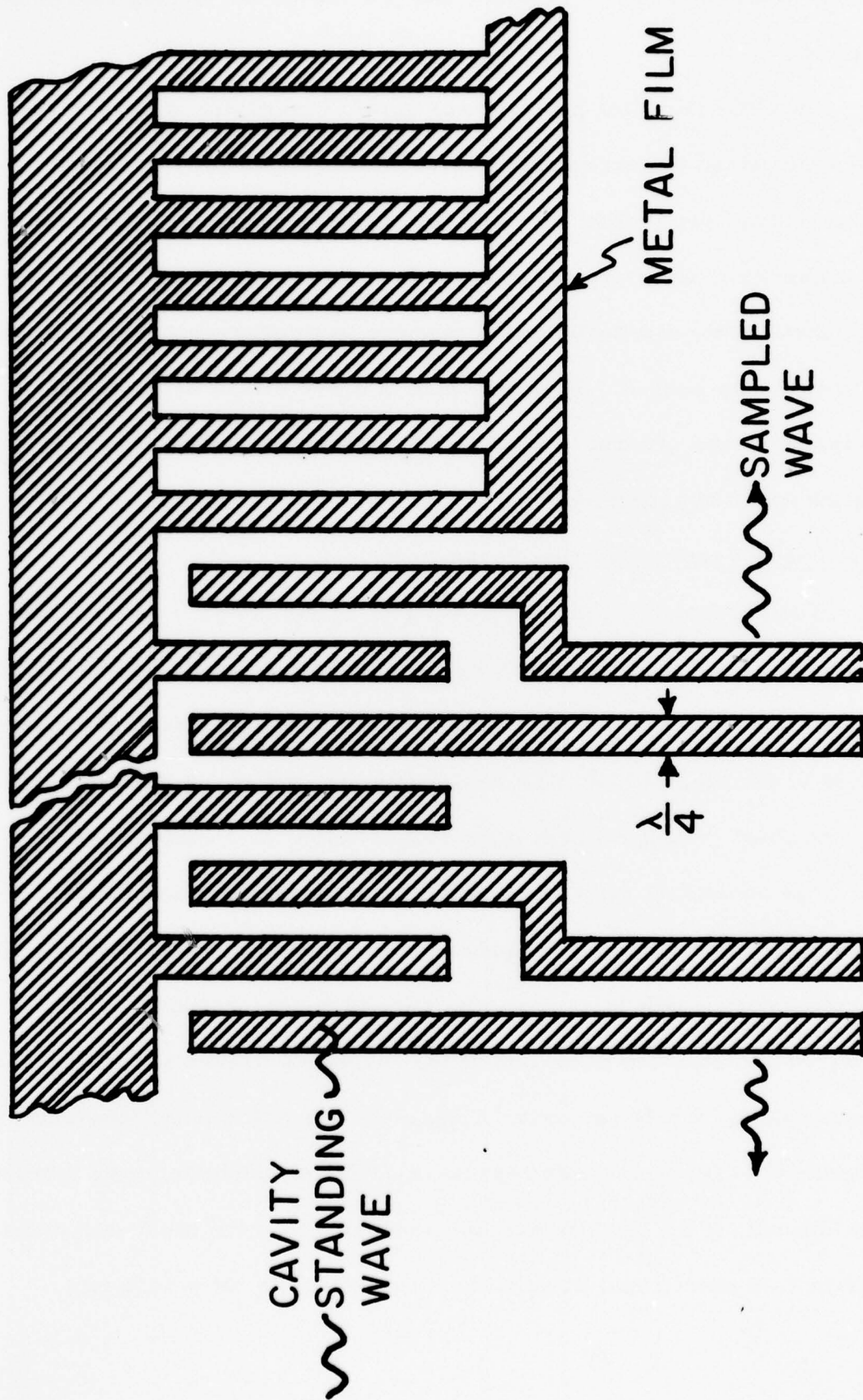


Figure 2.4 IDT Coupled Grating.

not perpendicular to the propagation path the cavity was leaking energy off to the sides.

Once the skew line problem was solved resonators of much higher Q were fabricated but not up to the value demonstrated previously. A careful study of the grating revealed that a periodic error is introduced by the lead screw of the stepping table and that the error caused the grating to become slightly non-periodic and thus the optimum resonance condition could not be approached. Since this kind of error cannot be corrected, even in the design, we had to abandon any attempt to fabricate gratings using the step and repeat system.

2.2.5 Phase Weighted Grating Resonators

The concept of a phase weighted grating resonator is new and was introduced in the proposal. Since we were ultimately unable to make gratings with the step and repeat system, and since the cost of one such commercial mask is of the order \$4000, this device was not studied any further. The phase weighted grating concept is described below for completeness.

The equivalent point of reflection in a grating is a function of frequency and this implies a frequency dependence of the total cavity length. Since the cavity length determines the allowed resonant modes, it is possible to increase the bandwidth of the resonance without lowering the Q . For example, in a bulk resonator if the plate could be thinned inversely proportional to frequency then resonance could be maintained over a broader bandwidth and, if the thinning process suddenly stops the resonator would go through its usual rapid transition. Of course it is not possible to

dynamically thin a bulk resonator. However, an equivalent process can be performed in the grating by changing the periodicity of the discontinuity as a function of position. This phase weighting technique has been well established for pulse compression filters.

For resonators it would be desirable to maintain the resonance condition over a wider frequency so that fewer elements would be required in a given implementation or design. The quantity of interest then is the phase condition for resonance

$$\varphi = n\pi \quad n = 1, 2, \dots$$

where

$$\varphi = 2\pi f_n \left(\frac{\ell_o}{V_s} + 2 \frac{\ell_r}{V_g} \right) \quad (2.1)$$

f_n = resonant frequency

ℓ_o = separation between gratings

ℓ_r = apparent reflection point

V_s = velocity between gratings

V_g = velocity within grating.

The basic requirement is that the phase must be independent of frequency for a broad resonance, $\Delta\varphi = 0$. Taking $V_s = V_g$ we obtain

$$\ell_r = \frac{n}{4} \frac{V_s}{f_n} - \frac{\ell_o}{2} \quad (2.2)$$

This equation implies that the reflection point must have a $1/f$ dependence as expected. The grating periodicity in the region near ℓ_r would have the

periodicity $\lambda_n = V_s / f_n$. Thus as l_r moves across the grating as given in (2.2) the local periodicity also varies as $1/f_n$. However, this variation cannot occur too rapidly because the reflection coefficient must be large. Since the reflection coefficient results from many small additions the phase coherence must be maintained over a large number of discontinuities. This property may be described by an equivalent number of discontinuities, N_{eq} .

$$N_{eq} = \frac{M}{2} \ln \frac{f_1}{f_2} \quad (2.3)$$

where

M = number of wavelength across the total cavity

\ln = denotes natural log

f_1 = end of chirp, highest frequency

f_2 = start of chirp, lowest frequency.

For small values of phase weighting we can define $\Delta f = f_1 - f_2$,

$f_n = f_2$, then for $\Delta f / f_n$ small

$$N_{eq} \approx \frac{M}{2} \frac{\Delta f}{f_n} \quad (2.4)$$

or

$$N_{eq} \approx \frac{1}{4} \frac{\Delta f}{\Delta f_n} \quad (2.5)$$

where Δf_n is the cavity mode frequency interval.

The length of the chirp region is given by

$$\Delta l = \frac{M}{2} V_s \frac{f_1 - f_2}{f_1 f_2}$$

In this configuration the chirp slope is fixed by the constraint that the cavity remain in resonance. As a result Δl depends on what value of N_{eq} is required to give a large enough reflection coefficient. To increase the absolute bandwidth the gratings are simply made longer. The first constraint on the cavity length is due to limits in mask size or crystal length.

From the equation for Δl , a time bandwidth product can be obtained,

$$\Delta t \Delta f = \frac{M}{2} \left(\frac{\Delta f}{f} \right)^2. \quad (2.7)$$

For a modest $\Delta f/f$ of 10% and $M = 1000$ the time bandwidth product would be less than two, a very realizable number.

The bandwidth of the phase weighted resonator is limited finally by the bandwidth of the central IDT. Buld mode generation has been suppressed by arranging the high frequency sections of the grating to initially intercept the wave.

2.2.6 Two Port Bulk Wave Filters

In the study of two port surface wave filters it is natural to compare the performance of these devices to the bulk wave counterparts. Of particular interest are the stacked crystal filter configurations where two bulk wave resonators are coupled via a common ground electrode [5-15], Figure 2.5. If designed properly, the common electrode offers no resistance to the propagation of waves and therefore the two cavities are tightly coupled. The outside walls act as perfect reflectors and consequently the insertion loss of the device is very low. Out of band the rejection is large due to the

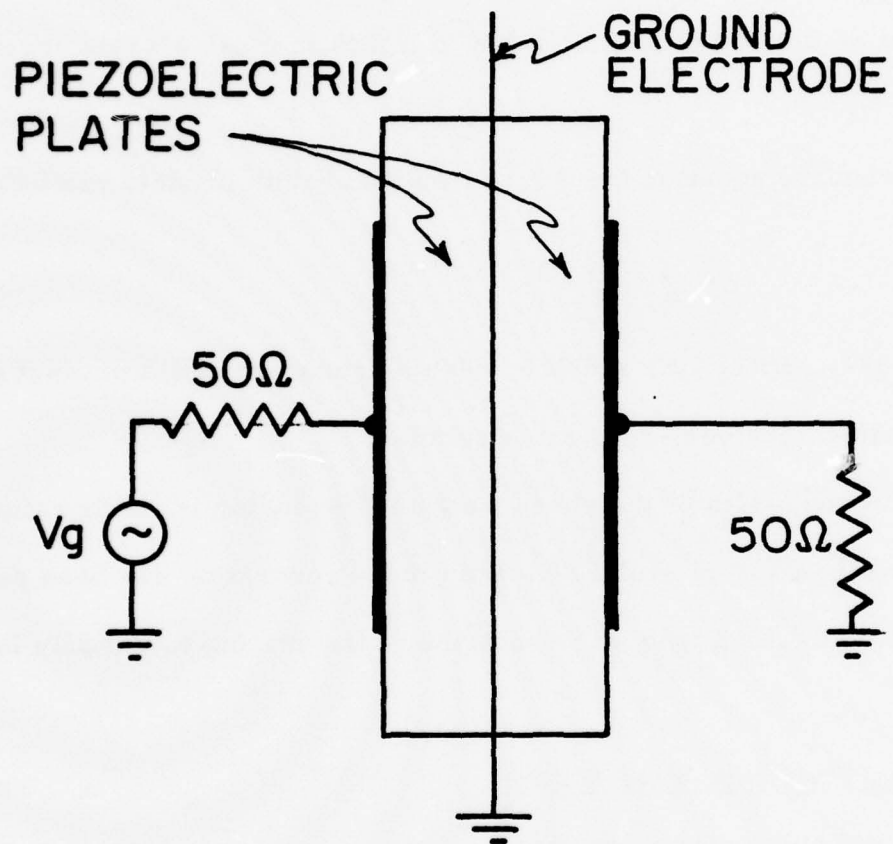


Figure 2.5 Stacked Crystal Filter Schematic.

high Q of the cavities and the electrostatic barrier between input and output electrodes. The stacked crystal filter is also a much smaller device since it is only one wavelength long for fundamental mode operation and at most five wavelengths at reasonable overtones whereas the SAW resonators are at least 300 wavelengths long.

During the last year of this project we began to look at the thin film stacked crystal filter as an alternate to the SAW resonator. Our task took two paths, first was a simple equivalent circuit modeling that drew upon our SAW modeling experience and second was a device fabrication geometry that appeared promising and could use the physical facilities developed on the program.

2.2.6.1 Crystal filter modeling. There are three basic approaches to analyzing the SCF configuration. The first method would be to treat it as a boundary value problem with excitation, the second is by the transmission line models treated exhaustively by Ballato [2], and the third by the use of Mason equivalent circuit modeling. The latter approach leads to simple SCF equivalent circuits whose simple pi network elements are readily describable in terms of resonator impedances or lumped elements. We show below that these lumped element descriptions clearly establish the filter characteristics in terms of material parameters readily available or obtainable from free plate resonator measurements including losses.

The Mason model approach studied on this program yields simple pi network models for the cases:

- (i) two perfectly coupled identical single mode or multi mode resonators having finite Q .
- (ii) two resonators coupled by a finite thickness bond region having arbitrary impedance and propagation loss.
- (iii) non-identical resonators coupled by finite bond region.

The case of multimode coupling due to boundary effects rather than direct piezoelectric excitation has not yet been attacked but should yield readily to the techniques already employed.

The analysis of the SCF using Mason equivalent circuits starts from the configuration of Fig. 2.6. In this derivation all impedances are expressed in electrical units normalized by $j\omega C^{-1}$ for convenience, and any mechanical impedance external to the transducer is normalized by the resonator impedance. The 1:1 ideal transformers need only be included in the external circuit analysis if the polar sense of the crystal and hence excitation phase of the wave need be known. A finite backing metalization may be included as an equivalent impedance or lumped inductance if thin.

In order to reduce the coupled circuit of Fig. 2.7a to a simple " π " or " T " equivalent, a sequence of $T \rightarrow \pi$ or $\pi \rightarrow T$ circuit transformations are performed. After each transformation the resultant network is expanded to include other series elements or shunt elements until a simple π network is obtained. For very many coupled resonators, the mathematical cascading technique used for SAW devices may be employed for analysis but does not result in an equivalent circuit in the usual sense.

The simplest SCF configuration is that of identical single mode disks

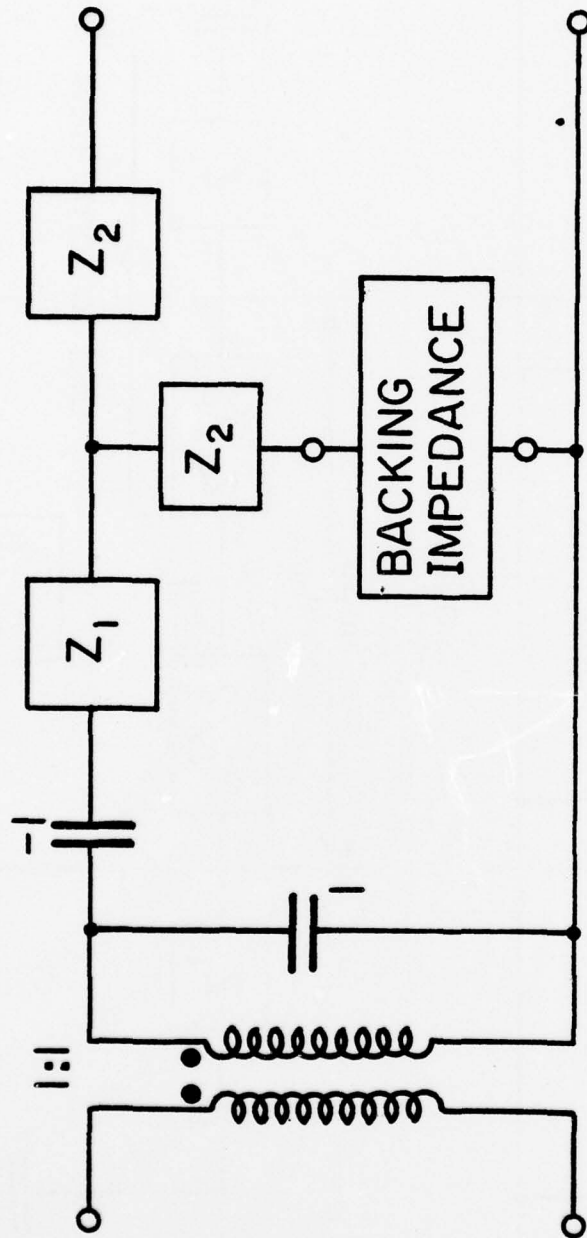


Figure 2.6 Mason Equivalent Circuit.

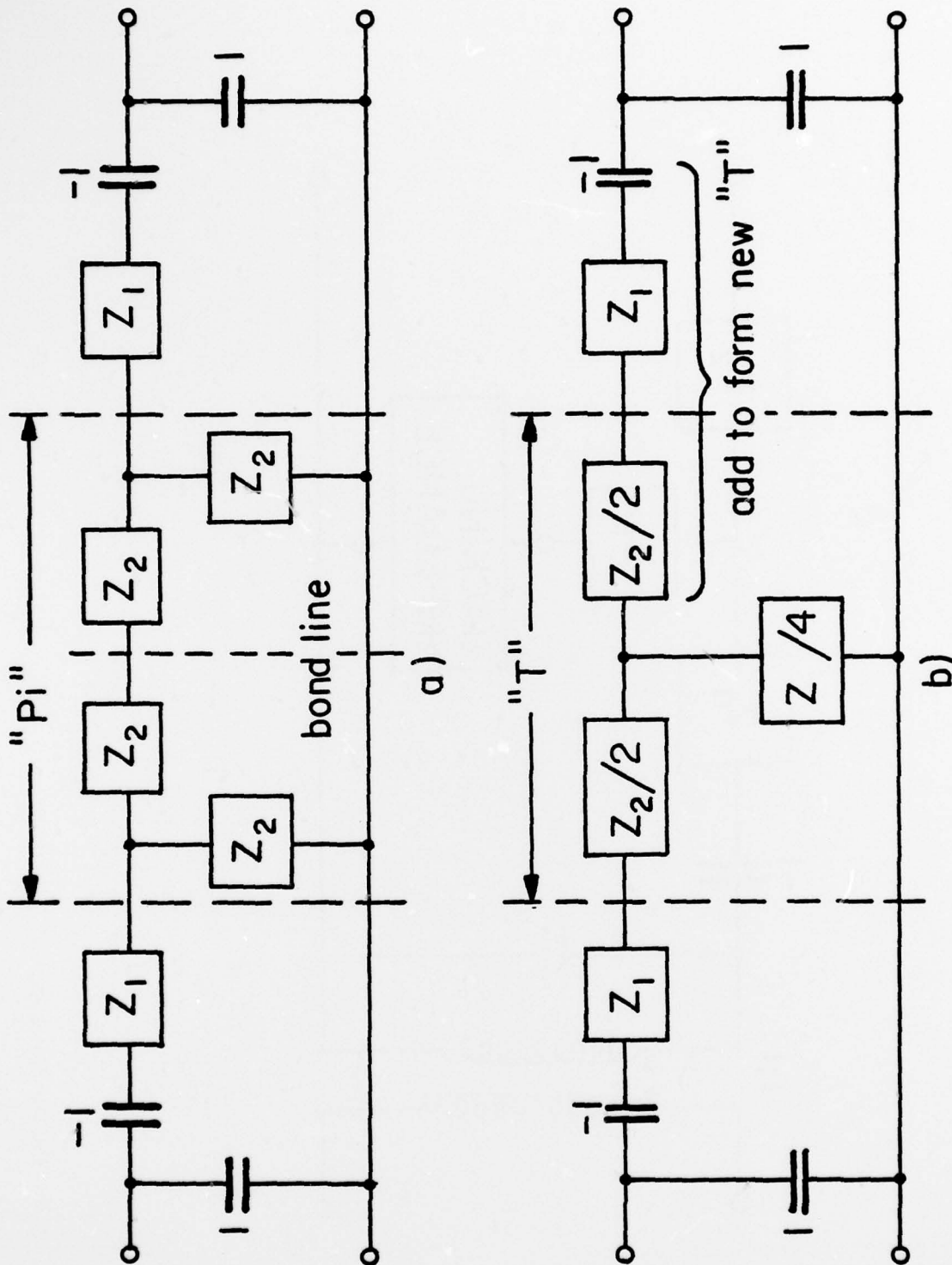


Figure 2.7 SCF with Zero Bond Thickness.

coupled by a zero thickness bond region. The resultant equivalent circuit is shown in Fig. 2.8. The impedances for the π elements are as follows:

$$Z_{R2} = \frac{1}{j\omega C} \left(1 - \frac{K^2}{\phi} \tan \phi \right)$$

$$Z_{R1} = \frac{1}{j\omega C} \left(1 - \frac{K^2 \tan \phi/2}{\phi/2} \right)$$

$$Z_C = j\omega C Z_P Z_{R2} (1 - \cot^2 \phi/2)$$

$$Z_P = \frac{\frac{-2}{j\omega C} \quad 2Z_{R1}}{\frac{-2}{j\omega C} + 2Z_{R1}}$$

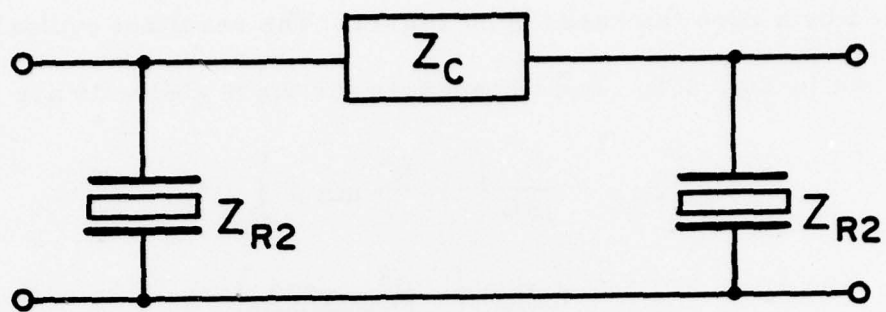
where

$$\phi = \pi f/f_0$$

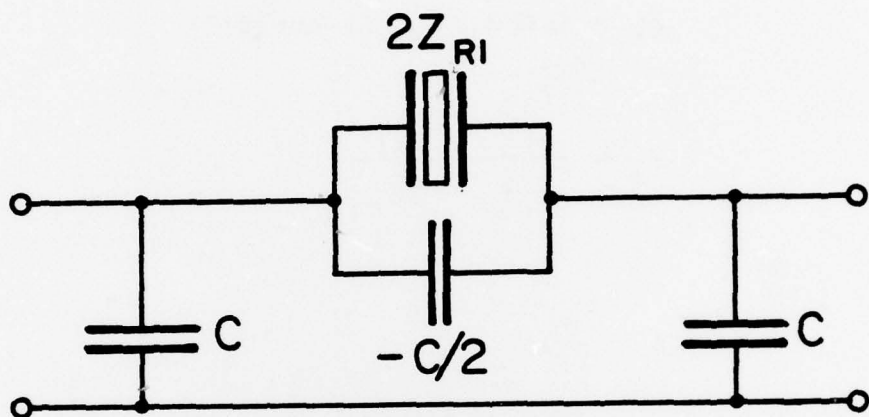
f_0 = parallel resonant frequency.

Note in particular that Z_{R1} and Z_{R2} are expressions for the impedance of individual resonators having parallel resonant frequencies of f_0 and $f_0/2$ respectively. Thus Z_{R1} is the impedance of the free resonator and Z_{R2} the impedance of a resonator having one free side and one clamped side. Any losses in the resonators may be accounted for by allowing the phase, ϕ , to be complex.

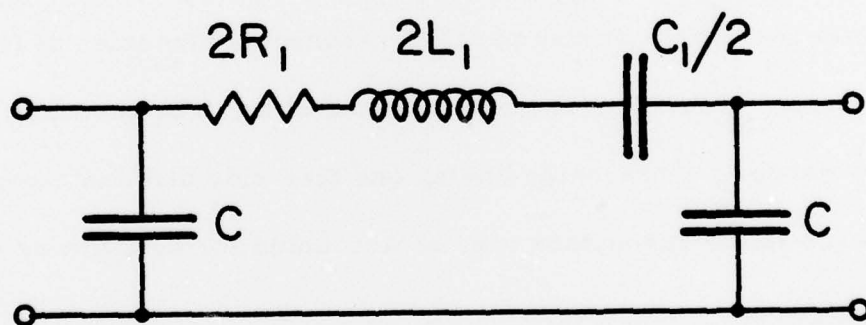
For frequencies near f_0 the impedance of Z_{R2} reduces to that of a capacitor C and Z_C reduces to Z_P , as shown in Figure 2.8b. The series element is now Z_P (which is $2Z_{R1}$ in parallel with a negative capacitor, $-C/2$). If the resonator is given its Butterworth-Vandyke equivalence, then the circuit of 2.8c results. This is a very simple result of considerable importance because the filter design constraints are simply related to



a)



b)



c)

Figure 2.8 Equivalent Pi Network for SCF.

single resonator performance. The series element of the π network in Fig. 2.8c is given exactly by

$$Z_C = \frac{2}{j\omega C} \left(\frac{\theta/2}{K^2} \cot \theta/2 - 1 \right)$$

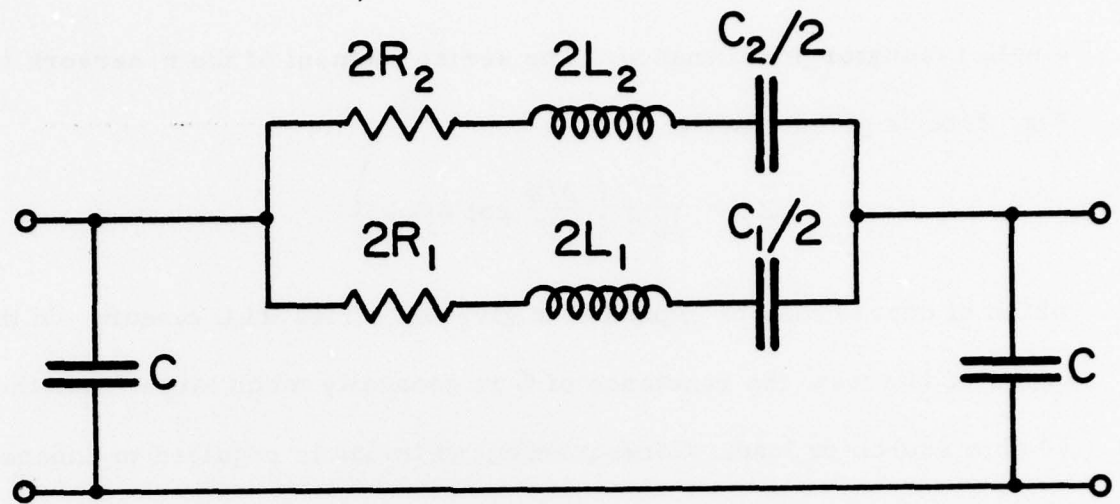
which of course may be expanded to give the series RLC circuit. In the cases of interest, the reactance of C is generally much larger than the 50 ohm source or load. Consequently, no tuning is required to enhance the conjugate impedance match when the resonator series loss is small. The transfer function of the circuit in Fig. 2.8c is virtually identical to that of a single resonator balanced bridge configuration. In each case the static capacitance is effectively subtracted from the resonator admittance leaving just the series RLC part.

The extension of Fig. 2.8c to more complicated cases should be evident. For example, multimode resonators would be represented by the circuit of Fig. 2.9a having additional RLC's in parallel and coupled resonators having slightly different resonant frequencies would have the circuit of Fig. 2.9b.

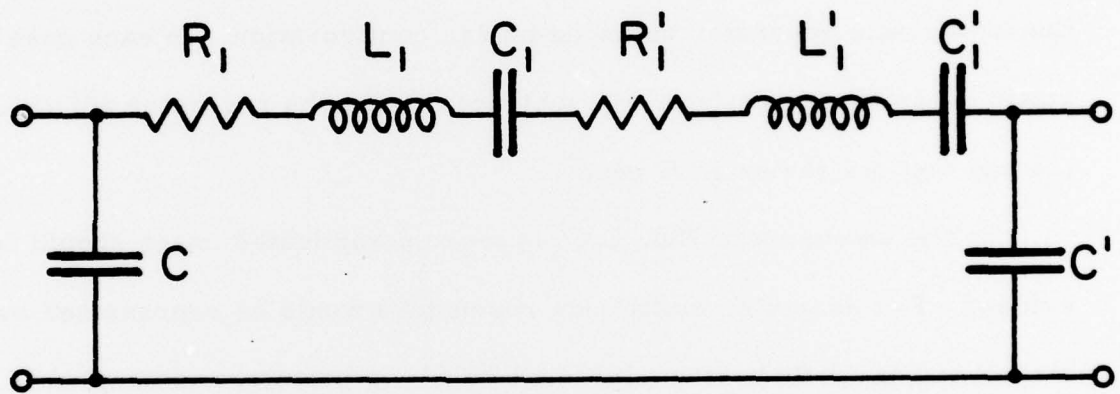
The case of two identical resonators coupled by a finite thickness bond region is of considerable technical interest because it relates directly to the experimental problem. The equivalent circuit for this configuration is identical to that in Fig. 2.8 except for the defining impedances:

$$Z_{R2} = \frac{1}{j\omega C} \left(1 - \frac{K^2 \tan \theta}{A_2 \theta} \right)$$

$$Z_{R1} = \frac{1}{j\omega C} \left(1 - \frac{K^2 \tan \theta/2}{A_1 \theta/2} \right)$$



a)



b)

Figure 2.9 SCF Lumped Equivalent Circuit.

$$Z_C = j\omega C Z_P Z_{R2} (1 - \cot^2 \phi/2) A_0 A_2$$

where

$$A_0 = 1 + a_0$$

$$A_1 = 1 + a_1$$

$$A_2 = 1 + a_2$$

$$a_0 = T_2 \frac{z^2}{2T_1(T_1 T_2 - z)}$$

$$a_1 = T_2 \frac{z T_1^2 (z - T_1 T_2)}{(T_1 + z T_2)(2T_1 T_2 - z)}$$

$$a_2 = T_2 \frac{T_1^3}{(1 - T_1^2)(2T_1 T_2 - z)}$$

where

$$T_2 = \tan \phi/2$$

$$T_1 = \tan \phi/2$$

$$z = z = Z_B / Z_T$$

We note that ϕ is the phase across the bond region and z is the normalized bond region impedance. For $\phi = 0$, $a_0 = a_1 = a_2 = 0$ and the circuit reduces to that of zero bond thickness derivation.

Also note that the filter transmission peaks at a series resonance of an equivalent resonator, Z_{R1} whose normal resonance is modified by the factor A_1 . For small bond thickness it is clear that the A 's may be expanded in the form of $1 + \epsilon$ where ϵ is a small number. The imaginary part of ϵ is the factor which introduces another series loss resistance in the series RLC circuit of Fig. 2.8c,

$$R_B = \frac{1}{\omega C} \frac{z \pi^2}{2K^2} \alpha \ell$$

where α is the propagation loss of the bond region, ℓ the bond thickness, and z the impedance ratio assuming the loss is small.

It is a general feature that all mechanical impedances are transformed by the proportionality factor $(\omega ck^2)^{-1}$ which gives high Q , but low k^2 and low capacitance materials, an unfavorable series loss resistance in to 50 Ω systems. For example, we measured a commercial 3.3MHz (3 pf.) quartz resonator and found its series loss resistance was 100 ohms as inferred by transmitting to a 50 Ω load. Two such resonators, perfectly bonded in a SCF configuration, would give 200 ohms at series resonance and an insertion loss of 9.5 dB. For an insertion loss of 1 dB or less a single resonator would require a series loss of 6.5 ohms or less implying a large resonator area at this low frequency.

2.2.6.2 Experimental device configuration. The experimental device configuration for the implementation of the SCF must be chosen carefully since one of the major experimental problems is the bond region between the two piezoelectric plates. The physical bonding of two piezoelectric plates is difficult except for thick plates and for that reason we elected to consider an approach using thin films rather than bulk crystals. The thin crystal films must, however, be supported in some manner in order to make the device practical. The substrate we have chosen is silicon because it can be selectively etched to form pockets, Figure 2.10. In Figure 2.10 the vertical dimensions are greatly compressed in order to show the transverse dimensions in some detail.

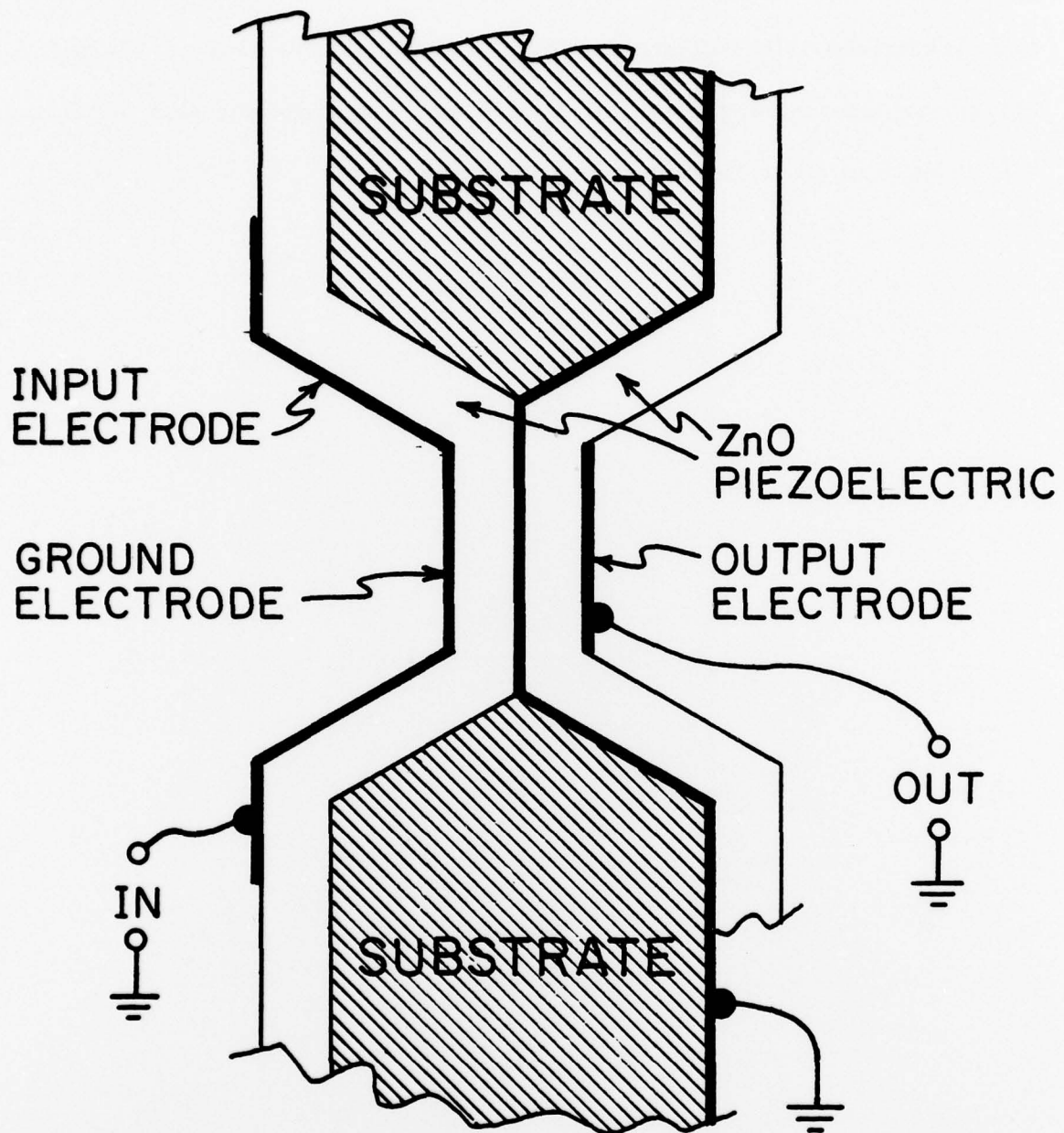


Figure 2.10 SCF, Crystal film implementation

Before the end of the program we had experimentally etched pockets in Si substrates using selective etching through oxide windows. We had clearly demonstrated the feasibility of Si as a substrate and plan to continue this project on other funding.

3.0 SUMMARY AND CONCLUSIONS

The major problems addressed during this research effort was the two port filter using SAW resonators and, during the last part of the program, the crystal film implementation of the stacked crystal filter. In order to carry out the SAW resonator device research, considerable effort was directed toward the problems of mask making, resonance measurements, and computational methods and display.

It was felt that a purely theoretical program was not in order because the theoretical modeling at USC had already been taken to the point where excellent results were being obtained. What was required then was a strong feedback from precise experimental measurements which could then influence the theoretical modeling. However, by the time the program got started much of the work originally proposed had already been reported by other researchers in this fast moving field. We decided then to place major emphasis on the two port resonator problem.

The experimental effort then hinged on the fabrication of some unique device geometries. To fabricate these devices we put together a step and repeat camera system for photomask production which would allow us to make the larger and more complicated devices.

The desired results were not obtained due to a number of reasons. First and perhaps most important, the photomask system lacked the needed precision and secondly there was a large turnover of inexperienced research personnel during the grant period which caused a lack of continuity in the program.

Late in the program the emphasis was shifted away from SAW devices to the bulk wave stacked crystal filter. This move was optimum because most of the mathematical modeling skills transferred easily from SAW to bulk wave, the step and repeat system was perfectly adequate to make the required photomasks, the computer controlled network could be employed in the measurements, and the device physics was more suitable for students not having one or two years training in the SAW area.

In conclusion, the two device configurations of interest, the phase weighted grating resonator and the in grating IDT coupling, are still valid concepts that were neither proved nor disproved by the results of this program. The introduction of the crystal film stacked crystal filter concept is of major importance because it shows a practical way to fabricate a device that has been most difficult to achieve by other means.

4.0 REFERENCES

1. E.J. Staples, "UHF Surface Acoustic Wave Resonators," Proc. 28th Annual Symp. In Frequency Control, U.S. Army Electronics Command, Ft. Monmouth, N.J., p. 280, (1974).
2. K.M. Lakin, T. Joseph, D. Penunuri, "A Surface Acoustic Wave Planar Resonator Employing an Interdigital Transducer," Appl. Phys. Lett. Vol. 25, No. 7, Oct. 1974, pp. 363-365.
3. T.R. Joseph, K.M. Lakin, D. Penunuri, "Surface Acoustic Wave Planar Resonator Using Grating Reflectors," Appl. Phys. Lett. Vol. 26, No. 2, Jan. 1975, pp. 29-31.
4. T.R. Joseph, K.M. Lakin, "Two-Port Cavity Low-Insertion-Loss Delay Line," Appl. Phys. Lett. Vol. 26, No. 7, April 1975, pp. 364-365.
5. "Transmission-line Analogs for Stacked Piezoelectric Crystal Devices," A. Ballato, Proc. 26th Annual Frequency Control Symposium, June 1972, pp. 86-91.
6. "Systematic Design of Stacked-Crystal Filters by Microwave Network Methods," A. Ballato, H.L. Bertoni, and T. Tamir, IEEE Trans., Vol. MTT-22, January 1974, pp. 14-25.
7. "Stacked-Crystal Filters," A. Ballato and T. Lukaszek, Proc. IEEE, Vol. 61, October 1973, pp. 1495-1496.
8. "A Novel Frequency Selective Device: The Stacked Crystal Filter," A. Ballato and T. Lukaszek, Proc. 27th Annual Frequency Control Symposium, June 1973, pp. 262-269.
9. "The Stacked-Crystal Filter," A. Ballato, Proc. IEEE Intl. Symposium on Circuits and Systems, April 1975, pp. 301-304.
10. "Distributed Network Modeling of Bulk Waves in Crystal Plates and Stacks," A. Ballato and T. Lukaszek, Technical Report ECOM-4311, May 1975, U.S. Army Electronics Command, Fort Monmouth, N.J. 07703.